# DYNAMICS OF AN ELECTRIFIED WATER/AIR INTERFACE SUBMITED TO AC VOLTAGE

**A. MOUKENGUE IMANO  S. NDJAKOMO ESSIANE**
Laboratoire EEAT, University of Douala, B.P. 8698 Douala, Cameroon, moukengue@univ-douala.com

**J. NDOUMBE  A. BEROUAL**
Laboratoire Ampère, CNRS UMR 5005, Ecole Centrale de Lyon, 69134 Ecully cedex, France,
abderrahmane.beroual@ec-lyon.fr

***Abstract:*** *A water droplet deposited on a conductor of high voltage transmission lines vibrates with a frequency proportional to the frequency of the applied AC voltage. The droplet also deforms subsequently under 50-Hz-voltage stress. Likewise, it has been observed that the surface of a water puddle on a high voltage conductor becomes unstable from a certain value of the electric filed strength, with respect to the geometry of the conductor or transmission line.*

*In this paper, the dynamics of a water/air interface is investigated theoretically when the electrode system containing the water droplet or water puddle is submitted to AC voltage. A mathematical model enabling us to simulate the axisymmetric deformations of droplets is used to calculate the critical electric field strength at which a water/air interface becomes unstable according to some approximation techniques, for a sessile water droplet on a metal electrode faced to rod electrode. Furthermore, this paper presents an experimental study of the deformation of a water droplet and water puddle on a plane electrode faced to another rod electrode to check the theory. Fundamental observations of current discharges characteristic of water/air interface are presented. The behaviour of the inception field strength of partial discharges between water/air interface and a rod electrode is also shown. The results of the investigations provide a better understanding of the approach to calculate the field inhomogeneity factor at the tip of a sessile water droplet.*

***Key words:*** *sessile droplet, water/air interface, droplet instability, electric field strength, discharge inception, discharge current.*

## 1. Introduction

The dynamics of the water droplets on high voltage transmission lines under AC voltage stress can produce complex dynamic shapes such as sideways wobbling and other modes of volumetric vibrations, as on the surface of the outdoor insulator. Furthermore, acoustic emissions from wet high voltage lines can reach locally unacceptable levels and are linked to energy loss from the lines [1]. It has been demonstrated that these acoustic emissions have their origin in electrical discharges from deformed water droplets on the lines, and these discharges depend principally on the electric field strength at each droplet surface. In effect, each deformed sessile droplet on a line conductor disturbs precisely the electric field along the conductor surface. This disturbance of the background field is attributed to the field enhancement at the deformed surface of each water droplet, which is a positive feedback phenomenon causing further distortion or vibration of the same droplet, when the line is submitted to AC voltage.

The dynamics of water droplets has been the subject of a certain number of experimental works, but only for water droplets on dielectric surface under electric stress. So far, and in our opinion, only few papers deal with experimental studies of the dynamic of conducting water surface submitted to ac voltage. Benjamin and Ursell [2] investigate theoretically and experimentally the stability of the plane free surface of water. Roero and Teich [1] also investigate experimentally the behavior of droplets on different high voltage conductors showing high framing rate records of their periodic deformation in the electric field. Finally, Lord Rayleigh [3] analyzed the equilibrium conditions for a conducting liquid in vertical electric field. His approximate treatment allowed him to determine a stable equilibrium shape for a conducting liquid under a given applied electric field strength.

The aim of this paper is to investigate the dynamics of an electrified water droplet and water surface. Precisely, we firstly use a mathematical model to calculate the theoretical electric field strength at the water/air interface, and secondly we experimentally regard the discharges initiation and development between water/air interface and metal electrode. The results of the investigation can provide a better understanding of the approach used elsewhere [4] to calculate the field inhomogeneity factor according to Schwaiger, and to determine the critical electric field strength at which the water/air interface becomes unstable using a virtual sphere according to G. I. Taylor.

## 2. The water/Air Interface Analysis

### 2.1. Description of the water/air interface

Let us consider a water droplet on a conducting flat surface (Metal electrode) subject to an AC electric field, as shown in Fig. 1. This water droplet always elongates in the direction of the field at a given time *t*. The metal electrode is smooth, horizontal and does not dissolve or react with the used water. The water/air, water/electrode and air/electrode interfaces conjoin at a so-called contact line. For the gas around the droplet and the used water, we are made the same considerations as in [5]: The air is a perfect dielectric steam, and water is conductive and incompressible.

When an AC electric field is applied to the sessile water droplet, its shape can change with respect to the polarity of the electric field. That means the droplet can vibrate [6] with or without elongation other motion.

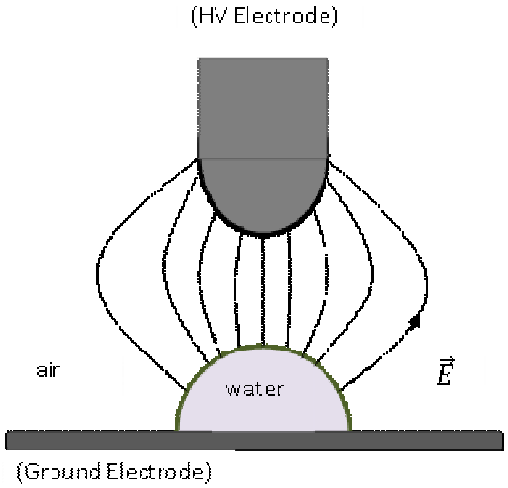


Fig.1 Electrode arrangement with a water droplet submitted to electric field

Let us consider the droplet vibration with or without elongation as a simple deformation of the droplet in the direction of the electric field. It is shown elsewhere [5] and by Iliev [7], that this deformation is a result of the change of the different interface energies, and the change of the negative work supply to the water/air interface and the contact line subjected to external forces due to the interfacial tension, the pressure difference, the electric stress, the effect of the viscosity and the gravity.

The reduction of the Gibbs free energy of both water/air interface and contact line towards zero enables us to obtain the main equation of the shape of the water/air interface $I_{WA}$ at the equilibrium state [4]

$$\gamma_{WA} \cdot \left(\vec{\nabla} \cdot \vec{n}\right) - \sum f_I = 0. \qquad (1)$$

Let us decompose the force balance given by equation (1) into normal and tangential components, according to Fig. 2. The interaction of all external and internal forces in the direction normal to $I_{WA}$ enables us to rewrite equation (1) in

$$\vec{n} \cdot \sum f_I = \vec{F}_p + \vec{F}_{En} + \vec{F}_{\mu n} + \vec{F}_g = \vec{F}_\gamma \qquad (2)$$

with

$$\vec{F}_\gamma = \vec{n} \cdot \gamma_{WA} \left(\vec{\nabla} \cdot \vec{n}\right) \qquad (3)$$

$$\vec{F}_p = -\vec{n} \cdot \Delta p \qquad (4)$$

$$\vec{F}_{En} = \vec{n} \cdot T_n \qquad (5)$$

$$\vec{F}_{\mu n} = \vec{n} \cdot 2\mu\vartheta_n \left(\vec{\nabla} \cdot \vec{n}\right) \qquad (6)$$

$$\vec{F}_g = \vec{n} \cdot g \cdot \Delta\rho \cdot z \qquad (7)$$

Contrary to the simplifications made elsewhere [5], the consideration of viscosity makes it possible to take into account the force interaction in the direction tangential to $I_{WA}$. According to G.I. Taylor [8], only the tangential components of the forces due to the electric stress and to the effect of the viscosity interact in the direction tangential to $I_{WA}$ of the droplet, thus equation (2) becomes

$$\vec{F}_{Et} + \vec{F}_{\mu t} = \vec{0} \qquad (8)$$

with

$$\vec{F}_{Et} = \vec{t} \cdot T_t \qquad (9)$$

$$\vec{F}_{\mu t} = \vec{t} \cdot 2\mu\vartheta_t \left(\vec{\nabla} \cdot \vec{n}\right) \qquad (10)$$

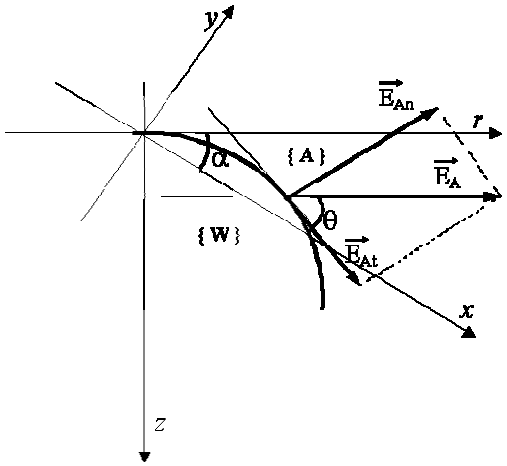


Fig. 2 Normal and tangential components of the electric field at the water/air interface in the surrounding air

## 2.2. Equations of the shape of the water/air interface

For generalization of results of the calculation, the system of the differential equations of the shape of $I_{WA}$ can be written in a non-dimensional form as [5]

$$\frac{d\theta}{dS} = \frac{1}{\left(1 - T_O \dfrac{\sqrt{X^2 + Y^2}}{t} \cos\theta\right)} (1 + A1) - \frac{\sin\theta + A2}{\sqrt{X^2 + Y^2}} \qquad (11)$$

$$\frac{dX}{dS} = \cos\theta \cdot \cos\alpha \qquad (12)$$

$$\frac{dY}{dS} = \cos\theta \cdot \sin\alpha \qquad (13)$$

$$\frac{dZ}{dS} = \sin\theta \qquad (14)$$

with

$A1 = B_O \cdot Z + W_{eO} \cdot \delta \cdot \cos^2\alpha \cdot \left(K_1 + K_2 \cdot \cos^2\theta\right)$

$A2 = \Omega_{eO} \cdot \delta \cdot t \cdot \cos^2\alpha \cdot \cos\theta$

S = *b*·*s*, X = *b*·*x*, Y = *b*·*y* and Z = *b*·*z*, where

- $b = \frac{1}{R_{Apex}}$ is the curvature at the origin of coordinates (Apex);
- $T_O = 13.76 \cdot 10^{-6} \cdot R_i$ is a time constant in s;
- $\Omega_{eO} = 44.21 \cdot E_{G\infty}^2$ is an electric parameter in $s^{-1}$ for homogeneous electric field and for a unit area ;
- $B_O = 67.23 \cdot 10^{-3} \cdot R_i^2$ is the non-dimensional Bond number;
- $W_{eO} = 3.08 \cdot 10^{-4} \cdot E_{G\infty}^2 \cdot R_i$ is the electric non-dimensional Weber number for homogeneous electric field and for a unit area ;
- $\delta = E_n^2 \cdot \cos^2(2\pi ft)$ is a non-dimensional variable parameter ;
- $E_n$ is a non-dimensional form factor for the electric field;
- $E_{G\infty}$ is the electric field strength of a homogeneous electric field in *kV*/c*m* , for a water temperature of 20°C;
- $R_i$ is the initial radius of the droplet in *mm*;
- $K_1 = 1$ and $K_2 = 78.18$ are non-dimensional electric constants;

### 2.3. Calculation of the form factor of the electric field at water/air interface

For a sessile droplet on a conducting solid surface, the deformed water/air interface enhances the initial electric field at its tip. This is a positive feedback phenomenon, which causes further distortion of the droplet. Furthermore and under certain conditions, the sessile water droplet can disintegrate or jump to the faced electrode

Let us materialize with *E* the electric field strength of the normal component of an electric field at one of the elementary points on the droplet tip. For a sessile droplet, as shown in Fig. 3, this electric field strength can be expressed as

$$E = \frac{U}{\eta(d-h)} = \frac{U}{d} \cdot \frac{1}{\eta\left(1-\frac{h}{d}\right)} \qquad (15)$$

$\eta$, *h*,*U* and *d* are respectively a corresponding inhomogeneity factor for the droplet-electrode configuration, the height of the droplet, a potential difference and the shortest distance between both electrodes. It is assumed that the water considered is conductive.

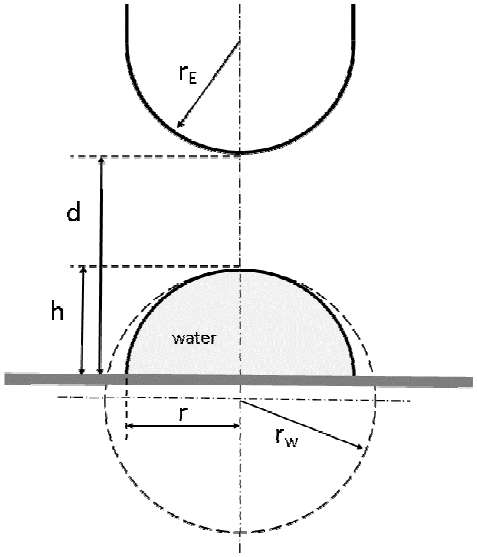


Fig.3. Top view of a droplet faced to rod electrode

Without water droplet, this electric field strength can be expressed as

$$E_0 = \frac{U}{\eta_0 d} \qquad (16)$$

$\eta_0$ *is* a corresponding inhomogeneity factor for the electrode-electrode configuration.

One defines in this case the electric form factor, as

$$E_n = \frac{1}{\eta\left(1-\frac{h}{d}\right)} \qquad (17)$$

for droplet-electrode configuration, and also

$$E_{0n} = \frac{1}{\eta_0} \qquad (18)$$

for electrode-electrode configuration without sessile droplet. The double influence of the geometry of the droplet on $E_n$ can be noticed. The first is directly through the height *h*, and the second is indirectly through the inhomogeneity factor $\eta$ calculated according to a (*p*, *q*) geometry of the configuration taken into consideration.

Let *R* and *r* be the radii of the major and minor spheres of a sphere-sphere configuration, respectively. The (*p*, *q*) geometry is defined by [9, 10]

$$p = \frac{d+r}{r} \text{ and } q = \frac{R}{r}. \qquad (19)$$

For the calculation of the form factor of the electric field at water/air interface, we consider two gap configurations:

- Sphere-sphere for water droplet faced to rod electrode with $p = \frac{d-h+r_W}{r_W}$ and $q = \frac{r_E}{r_W}$;

▪ Sphere-plane for water surface faced to rod electrode and to point electrode with $p = \frac{d - h + r_E}{r_E}$ and $q = \infty$.

To calculate $\eta$ for the sphere-sphere configuration, we assimilate the radius of curvature at the tip of the droplet to a virtual sphere according to G. I. Taylor [8].Moreover, a small water droplet can roughly be regarded here as having the form of a cap of ellipsoid of revolution [4]. Since the droplet deformation modifies the distance *d* - *h*, which in turn influences the field, $E_n$ will have to be determined by an iterative computation. The necessary algorithm is given in Table 1.

Table 1

Necessary algorithm for iterative computation of $E_n$

| *Step* | *Related actions* | *Related equations for the droplet tip* |
|---|---|---|
| 0 | Initialization | $E_n(1) = 1,\ d$ |
| 1 | Begin an iterative loop | $r(n+1)$ and $h(n+1)$ |
| 2 | Calculate the ellipticity | $e(n+1) = \left(1 - \frac{(r(n+1))^2}{(h(n+1))^2}\right)^{\frac{1}{2}}$ |
| 3 | Calculate the principal radii of curvature at the droplet tip, according to [24] | $r_W(n+1) = h(n+1) \cdot (\alpha(n+1)$ with $\alpha(n+1) = 1 - (e(n+1))^2$ |
| 4 | Calculate the distance between the droplet tip and the faced electrode | $a(n+1) = d - h(n+1))$ |
| 5 | Calculate the non-homogeneity factor | $\eta(n+1) = f(r_W(n+1), a(n+$ |
| 6 | Calculate the form factor and check for its convergence. Stop if not converged. If converged, go to step 1, up to a given *n* and store the calculated value. | $E_n(n+1) = f(\eta(n), h(n))$ |

As explained in our former works [4, 5], the Volume of the droplet is supposed to be constant, during the deformation of the droplet. In our case, the deformation of the sessile water droplet is also characterized by the variation in the radius r and the height h of the droplet. While admitting this observation also for a sessile droplet on a conducting smooth surface, and according to Leibniz [11], we can write and solve following equation:

$$5h^3 + 3rh^2 + \frac{\nu}{r}h + \nu = 0, \qquad (20)$$

with $\nu = \frac{3V_W}{\pi}$. and $V_W$ the volume of the water droplet.

To determinate $E_n$ for the water surface and electrode configuration, it was assumed that the deformation of the water surface had only a neglected influence on the distance between electrode and water surface. In our case, the inhomogeneity factor according to Schwaiger [12] can be approximated to

$$\eta = a^{-0,904}, \qquad (21)$$

for droplet faced to rod electrode, with *a* the spacing between the droplet tip and the opposed rod electrode in mm.

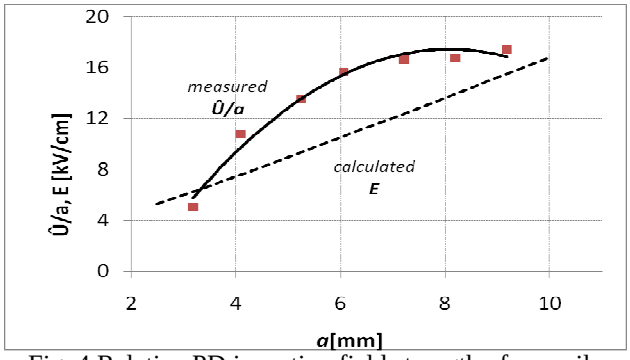


Fig. 4 Relative PD inception field strength of a sessile droplet versus spacing (*a*) and corresponding calculated field strength, for rod electrode.

### 2.4. Numerical results of the calculated critical electric field strength

#### 2.4.1. Water droplet on plate electrode faced to rod electrode

The numerical results presented in this paper were obtained for a droplet with an initial radius $R_I$ of 3 *mm*, and the calculation was only done for a sphere-sphere configuration. At begin of the calculation, the developed numerical routine considers automatically the electric form factor $E_n$ = 1 to reduce the still more computational costs. It is also well known that the form factor depends on the shape of the droplet under voltage stress. For the computation of the shape of the droplet under voltage stress, we used the same method as in [4, 5] to solve the system of equations formed by Eqs. (11) to (14). In our developed MATLAB routine, we consider that air have a dielectric strength of 30 kV/cm under normal conditions and $r_E$ = 5 mm. The obtained result of the calculated electric field strength is illustrated in Fig. 4, with comparison to the experimental determined field strength.

#### 2.4.2. Water surface faced to rod electrode

Fig. 5 illustrates the calculated electric field strength for water surface faced to rod electrode as a function of the distance between the water surface and the opposed

electrode. These results of calculation were compared to experimentally determined electric field strength for corresponding configurations. In our case, we have considered in the calculation that water/air interface does not move. Therefore, the form factor of the electric field will not have to be determined by an iterative computation. For the calculation of $E_n$ and the electric field strength, we consider the sphere-plate configuration. The problem has been solved for

- $r_E$ = 5 mm
- the dielectric strength for the surrounding air = 30 kV/cm.

In our case, the electric field strength at water/air interface, according to Schwaiger [12] for no deformable water/air interface, can be approximated to

$$E = \alpha_1 a^2 + \alpha_2 a + \alpha_3, \qquad (22)$$

for water surface faced to rod electrode, with: $\alpha_1 = 2 \cdot 10^{-2}$ kV/cm·mm$^2$, $\alpha_2$ = 3,7 kV/cm·mm and $\alpha_3$ = 3,3 kV/cm, *a* in mm.

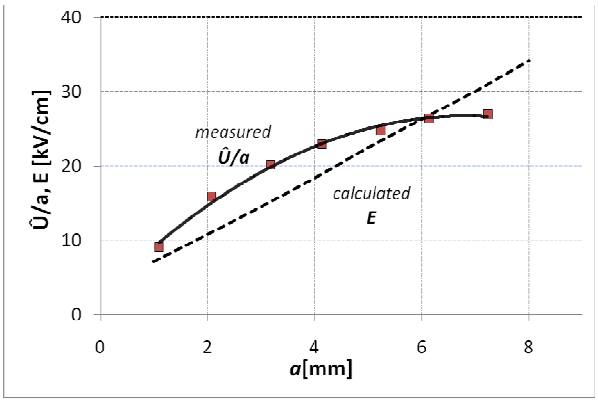


Fig. 5 Relative PD inception field strength for a water/air interface versus spacing (a) and corresponding calculated field strength, for rod electrode.

## 3. Experimental Study of the Dynamic of Water/Air Interface

In the preceding paragraph, we showed through descriptions and mathematical formulations that water/air interface is distorted when submitted to an electric field. We also calculated the electric field strength at water/air interface faced to a metal electrode. In order to verify these results, we studied qualitatively the dynamics of a sessile water droplet on metal electrode and a conducting water surface submitted to AC voltage.

### 3.1. Experimental setup

A simple set-up has been used to study the behaviour of water/air interface under AC voltage stress, as in the case of sessile droplets on the high voltage liens [13, 14]. Fig. 6 shows the completed experimental setup with an electrodes arrangement. The rod electrode is connected through a high voltage resistance ($R_p$) of 100 MΩ to the AC high voltage source and the plate electrode connected to ground.

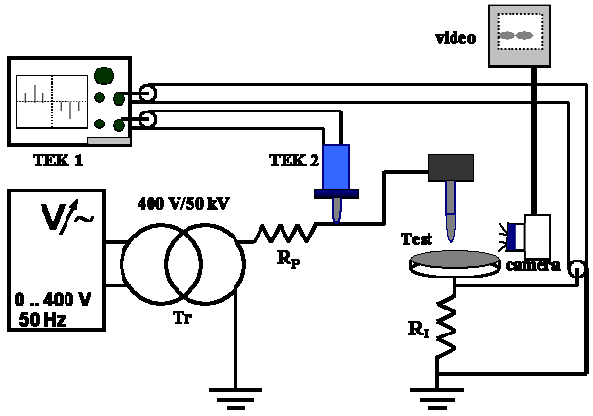


Fig. 6 Experimental setup

For the water droplet and generally water surface, we used normal drinking water with a conductivity of 320 µS/cm. The volume of the droplet was 50 µl. This sessile droplet was placed on the surface of a metal plane electrode with the help of a glass syringe, as shown in Fig. 7 for rod-plane electrode arrangement. Furthermore, for the flat water surface configuration we used a specially shaped electrode which is made of stainless steel and which can contain up to10 ml water, as shown in Fig. 8 with rod electrode.

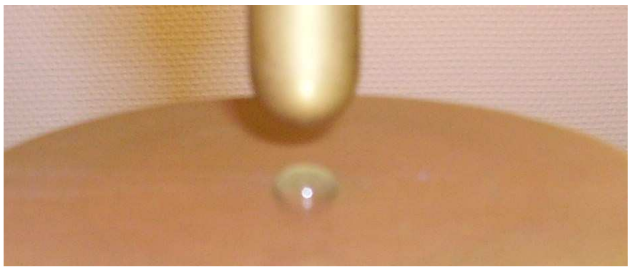

Fig. 7 Water droplet in rod-plane electrode arrangement.

The applied AC voltage on the electrodes arrangement is measured using a Tektronix P6015A high voltage probe (TEK 2). The potential drop across the resistance $R_I$ (75 Ω, 1/4 W) fed directly to the digital storage oscilloscope (Tektronix, TEK 1) to measure the discharge current characteristics. AC voltage was supplied from a single phase 230 V/50 kV test transformer. The behaviour of the drop surface or water surface was recorded by using a CCD-IRIS video camera.The 50-Hz-voltage was increased gradually until the first partial discharges (PD) occurred. The exact value of the PD inception voltage and the voltage shape were recorded with a digital storage oscilloscope (Tektronix). The measurements for the determination of the PD inception field strength have been evaluated according to the proposed method of IEC 60060/2. It is assumed that all experiments are normally distributed (with 95 % confidence interval of the expected values, in our case).

Fig. 8 Water surface with the rod electrode.

## 3.2. Results and discussion

### 3.2.1. The PD initiation field strength for a conducting sessile droplet faced to metal electrode

The initiation voltage of the partial discharges (PD) between a droplet surface and metal electrode ones depends on the initial geometry and a further deformation of the droplet. Fig. 4 shows the behaviour of the PD inception field strength of the droplet surface faced to the rod electrode, with respect to spacing. In the same figure, the corresponding calculated electric field strength is compared to the measured PD inception field strength.

The experimentally determined field strength gives the critical condition for the stability of the water/air interface, and is observed for spacing up to 7.23 mm. It can also be observed, that for relative small gap distances the water/air interface surface will become quickly unstable. However, the calculated corresponding electric field strength does not completely behave with spacing *a* like the PD initiation field strength. This difference is due to approximation method used for the calculation. But, the disagreement between both experimentally and theoretically obtained results is related to spacing *a*. The dielectric characteristics of air, for instance the mechanism related to discharge initiation and development in air, have certainly significant influence on experimental results for large distances between droplet surface and opposed rod electrode. These characteristics were not considered in the calculation of the critical electric field strength. In effect, in our theory the air is a perfect dielectric steam.

### 3.2.2. The PD initiation field strength for a conducting water surface faced to metal electrode

A water surface can become unstable when subjected to an electric field and when the field strength reaches the relative critical value. For the considered experimental arrangement, the initial field strength is imposed by the geometry of the opposed metal electrode. The mechanism which comes into play under these conditions is the electrostatic deformation of the water/air interface. This was observed for spacing up to 9.18 mm. Below this spacing, PD initiation field strength is generally found to be lower for the rod electrode, as shown in Fig. 5. Nevertheless, the water surface will become unstable for lower field strengths with point electrode as well as with rod electrode. The agreement of the calculated electric field strength with the measured PD initiation field strength was only partially satisfactory. In effect, the PD initiation field strength will become constant or will decrease for $a > 5$ mm.

### 3.2.3. The instability of the water/air interface

A potential $\hat{U}$ of up to $= \pm 15$ kV could be applied to the water drop by means of a continuously variable power supply. Higher values of potential tended to cause the water/air interface to become unstable or a water droplet to move up from plane electrode to rod electrode. The camera presented in Fig. 6 enabled us to observe and film the droplet and the water surface before and after the course of each experiment. The experiments were performed for five different distances from the top of the droplet (or water surface) to the faced electrode: 3.18 mm, 4.14 mm, 5.24 mm, 6.13 mm and 7.23 mm.

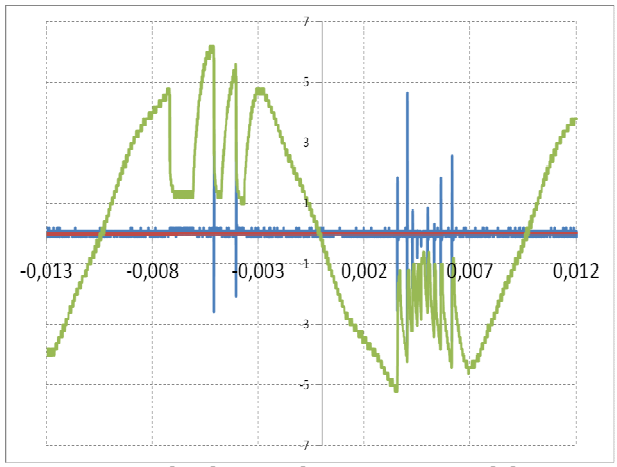


Fig. 9 Typical voltage and current measured during a discharge development for a water/air interface at spacing of 3.18 mm to the rod electrode.

The behaviour of the recorded voltage and current illustrates clearly the dynamic of water/air interface. All recorded results show that when the applied voltage reached a certain value, a current began to flow between the metal electrode and the droplet or water surface. This current can become stabile (established current) or unstable (impulse current). Fig.9 illustrates the typical behaviour of voltage and discharges current observed when the water surface is subjected to 50-Hz electric field for both point and rod electrodes. The instability of water/air interface is thereby evidenced through the flow of impulse current in the gap due to corona discharges on the water surface. This instability is also characterised by the vibration or motion of the water/air interface.

## 4. Conclusion

It has been shown how a simple mathematical model can be used to predict the dynamics or the stability of a water/air interface, and an experiment has been described which approximately confirms the theory under certain conditions with respect to the dimensions of the system used. We also apply the theories of Schwaiger and G.I. Taylor to calculate values of the field strength which can initiate the instability of the water/air interface. However, the relative small dimensions of our system compared to Schwaiger's experiments are not a negligible obstacle to the calculation of the field strength at the water/air interface with higher precision.

The dynamics of the water droplet on a conducting solid surface, and also of the conducting water surface, is hereby evidenced through the flow of impulse current in the gap due to corona discharges at the water/air interface. Furthermore as expected, the obtained results also enable us to affirm, that the electric field applied to the water/air interface is controlled by the electrode geometry and spacing between water surface and the electrode..

## 5. Acknowledgments

The authors would like to thank the Ecole Centrale de Lyon (France) for the financial support.

## References

1. Roero, C., Teich, T. H.: *Water drops on high voltage transmission lines*, Electrostatics Society of America (ESA) Annual Meeting University of Alberta, Edmonton, Canada, 2005.

2. Benjamin, T.B., Ursell, F: *The stability of the plane free surface of a liquid in vertical periodic motion*, Journal of Colloïd and Interface Science, Proceeding of the Royal Society, A, vol. 280 (1964), 505-515.

3. Lord Rayleigh: *On the Equilibrium of Liquid Conducting Masses charged with Electricity*, Phil. Mag. , 14, 184, 1882.

4. Moukengué Imano, A., Beroual, A.: *Deformation of water droplets on solid surface in electric field Simulation of the shapes of a water droplet on insulated solid surface in an AC electric field*, Journal of Colloïd and Interface Science, vol. 298, 2006, pp. 869-879.

5. Moukengué Imano, A., Ndjakomo Essiane, S., Beroual, A: *Simulation of the shapes of a water droplet on insulated solid surface in an AC electric field*, Canadian Journal of Physics, Issue 85, 2007, pp. 1-17.

6. Higashiyama, Y., Tamagata, T., Sugimoto, T.: *Vibration of water droplet located on hydrophobic sheet under the tangential AC field*, Industry Application Conference, 1999. Thirty-Fourth IAS Annual Meeting. Conference Record of the 1999 IEEE, Vol. 3, pp. 1825-1830.

7. Iliev, S. D.: *The effects of resistance to shift of the equilibrium state of a liquid droplet in contact with a solid*, Journal of Colloid and Interface Science 213, 1999, 1-19.

8. Taylor, G. I.: *Disintegration of water drops in an electric field*, Proceeding of the Royal Society, A, vol. 280 (1964), 383-397.

9. Bresson, C. : *Appareillage électrique haute tension : Théorie – Construction - Applications*, Dunod, 1930.
10. Bayer, M., Boeck, W., Möller, K., Zaengl, W.: *Hochspannungstechnik*, Springer Verlag, 1986.

11. Kangas, S.: Manitoba Math Links, volume 1I, issue #1, Published by the Department of Mathematics, University of Manitoba, 2001.

12. Schwaiger, A.: *Elektrische Festigkeitslehre*, Springer-Verlag Berlin, 1925.

13. Roero, C., Teich, T. H., Weber, H-J.: *Mechanical and associated discharge behaviour of sessile water drop*, Proc. of 15th Int. Conf. on Gas Discharges and their Applications, Toulouse, France, 2004, Vol.1, 335-338.

14. Straumann, U., Semmler, M.: *About the mechanism of tonal emission from high voltage lines*, Proc. of 15th Int. Conf. on Gas Discharges and Their Applications, Toulouse, France, 2004, Vol.1, 363-366.